JOURNAL OF CATALYSIS **103**, 224–227 (1987)

In Situ Laser Raman Spectroscopy of Nickel Oxide Supported on γ-Al_2O_3

Recent *in situ* laser Raman spectroscopy (LRS) studies revealed that crystalline oxides (3-dimensional oxide phases) and supported metal oxides (2-dimensional oxide phases) exhibit different responses to thermal treatments in a controlled environment of dry air (*1, 2*). For crystalline oxides the thermal treatment is reversible and only thermal broadening of the metal–oxygen Raman bands are observed at elevated temperatures. The peak positions of the Raman bands for the crystalline oxides are constant during the thermal treatment. The response of supported metal oxides (atomically dispersed metal oxides coordinated to the surface of an oxide support) to the same thermal treatment is very different than that observed for crystalline oxides. For the supported metal oxides the thermal treatment is *not* reversible, and the most intense metal–oxygen Raman band simultaneously *sharpens* and *shifts* to higher frequency at elevated temperatures. Only upon the addition of water vapor at room temperature to the supported metal oxides does the Raman band shift back to lower frequency and broaden to its original state. The very different response of the Raman band of the supported metal oxides to thermal treatment is due to the coordination of water molecules to the highly dispersed supported metal oxides from prior exposure to ambient conditions (*1–4*). During the *initial* thermal treatment the water molecules coordinated to the supported metal oxides desorb and this causes the Raman band to simultaneously sharpen and shift to higher frequency. The removal of the coordinated water molecules from the supported metal oxide species decreases the degree of disorder (the density of states) and affects the symmetric M=O stretch (*1, 3, 4*). Once the water vapor is desorbed from the supported metal oxides, the *subsequent* thermal treatments in dry air are reversible, and only slight thermal broadening of the Raman band is observed at elevated temperatures (*1*). The supported metal oxides previously examined for the effect of water vapor upon the Raman bands are tungsten oxide, molybdenum oxide, vanadium oxide, rhenium oxide, and chromium oxide (*1–6*). In these Raman studies the metal oxides were supported on γ-Al_2O_3 and TiO_2. All of these supported metal oxides exhibit strong Raman bands at ~900–1100 cm^{-1} which have been assigned to the symmetric stretch of the terminal M=O bonds (*7*). Another common feature of the supported metal oxides listed above is that they all possess high oxidation states when oxidized (W^{6+}, Mo^{6+}, V^{5+}, Re^{7+}, and Cr^{6+}). There is no *in situ* Raman data in the literature about supported metal oxides on γ-Al_2O_3 and TiO_2 that possess low oxidation states (Ni^{2+}, Cu^{2+}, and Co^{2+}). In the present study we report the first *in situ* laser Raman data for nickel oxide supported on γ-Al_2O_3.

The 13% nickel oxide on γ-Al_2O_3 (Harshaw, ~180 m^2/g) sample was prepared by the incipient wetness impregnation method by adding an aqueous solution of nickel nitrate to the alumina powder. The catalyst was subsequently dried at 110°C and calcined in air at 450°C for 16 h. The accuracy of the nickel content was further verified by atomic emission spectroscopy. Bulk NiO was prepared by calcination in air of $Ni(NO_3)_2 \cdot 6H_2O$ at 450°C for 16 h, and bulk $NiAl_2O_4$ was prepared by calcination of a stoichiometric amount of $Ni(NO_3)_2 \cdot 6H_2O$ and γ-Al_2O_3 at 870°C for 24 h. Powder

0021-9517/87 $3.00

X-ray diffraction patterns (Philips diffractometer using Cu *Kα* radiation and diffracted beam monochromator) confirmed the crystalline nature of the NiO and $NiAl_2O_4$ samples.

A detailed description of the *in situ* multichannel laser Raman spectrometer setup has been given elsewhere (*8*, *9*). The 514.5-nm line of an argon ion laser was used for excitation with power at the sample location up to 40 mW. About 0.2 g of sample material was first pressed under 10 kpsi into a 13-nm-diameter wafer and was mounted on a stationary quartz stage capable of *in situ* treatments up to 600°C during spectral measurements. A triple monochromator was coupled to an optical multichannel analyzer equipped with a cooled intensified photodiode array detector for signal averaging. The Raman signals of the nickel oxide samples were intrinsically weak, and each spectrum was recorded with 10 min of accumulation time. The overall spectral resolution was about 6 cm^{-1}.

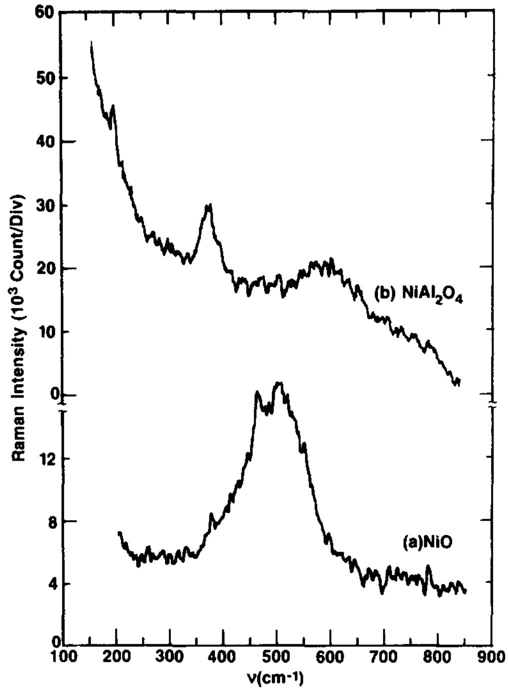

FIG. 1. Laser Raman spectra of bulk oxides: (a) NiO and (b) $NiAl_2O_4$.

The laser Raman spectra for unsupported $NiAl_2O_4$ and NiO are presented in Fig. 1 in the range 150–850 cm^{-1}. NiO has a defect NaCl structure with Ni in octahedral sites, and $NiAl_2O_4$, formed by the solid state reaction between NiO and Al_2O_3 at elevated temperatures, has an inverse spinel structure with Ni in octahedral and tetrahedral sites (*10*). The crystalline NiO exhibited two broad and overlapping Raman bands at 460 and 500 cm^{-1}, and crystalline $NiAl_2O_4$ possesses Raman bands located at 200, 375, and 600 cm^{-1}. The crystalline $NiAl_2O_4$ Raman band at ~375 cm^{-1} is unique to this phase and its presence in a Raman spectrum identifies the presence of crystalline $NiAl_2O_4$.

The *in situ* laser Raman spectra of 13% NiO/Al_2O_3 are shown in Fig. 2 as a function of treatment temperature in dry air. Raman bands were not present in the region 900–1100 cm^{-1} for these samples and suggest that M=O bonds are not present in the $NiO–Al_2O_3$ system (*7*). The Raman band for the supported nickel oxide on γ-Al_2O_3 at room temperature (Fig. 2a) is different than the Raman band for crystalline NiO (Fig. 1a) and $NiAl_2O_4$ (Fig. 1b). The supported nickel oxide exhibits a Raman band at ~550 cm^{-1} and does not possess the crystalline NiO Raman bands at 460 and 500 cm^{-1} or the crystalline $NiAl_2O_4$ Raman bands at 200, 375, and 600 cm^{-1}. The supported nickel oxide phase also exhibits reduction characteristics that are very different from crystalline NiO and $NiAl_2O_4$. Temperature programmed reduction (TPR) experiments showed that the reduction of the supported nickel oxide phase was significantly retarded relative to crystalline NiO, but was significantly more facile than the reduction of crystalline $NiAl_2O_4$ (*11*). The LRS and TPR data reveal that the supported nickel oxide phase is distinctly different than crystalline NiO and $NiAl_2O_4$. In addition, X-ray photoelectron spectroscopy (XPS) examination of the supported nickel oxide on alumina showed that the nickel oxide was highly dispersed as Ni^{2+} on the alumina

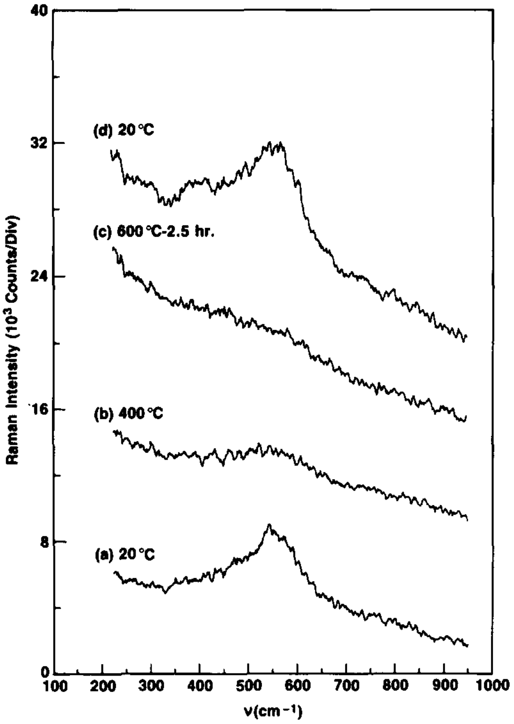

FIG. 2. *In situ* laser Raman spectra of 13% NiO/Al_2O_3 (previously calcined at 450°C): (a) 20°C, (b) 400°C, (c) 600°—2.5 h, (d) 20°C—post *in situ* calcination.

support (*11*). The combined LRS, TPR, and XPS data suggest that the supported nickel oxide is highly dispersed as a surface oxide and strongly interacting with the alumina support. Upon heating the 13% NiO/Al_2O_3 sample to 400 and 600°C only thermal broadening of the supported nickel oxide Raman band is observed (Figs. 2b and c). Cooling the 13% NiO/Al_2O_3 sample down to room temperature restores the ~550 cm^{-1} Raman band for the surface nickel oxide on the alumina support (Fig. 2d). In addition, there is a small Raman band at ~375 cm^{-1} characteristic of $NiAl_2O_4$ after the 2.5-h treatment at 600°C (Fig. 2d). This thermal treatment apparently converted a very small amount of the supported nickel oxide to $NiAl_2O_4$.

The response of the Raman band of the surface nickel oxide in the 13% NiO/Al_2O_3 sample to thermal treatment is very different than that previously observed for supported metal oxides present as surface oxides coordinated to the oxide support. The Raman band for the surface nickel oxide did *not* sharpen and shift to higher frequency as previously observed for the surface metal oxides (W, Mo, V, Re, and Cr) (*1–6*). Instead, the surface nickel oxide Raman band at ~550 cm^{-1} only exhibited a pronounced thermal broadening at elevated temperatures and the thermal treatment was reversible (except for the minor amount of $NiAl_2O_4$ formation). The crystalline NiO Raman bands at 460 and 500 cm^{-1}, however, do not exhibit such pronounced thermal broadening (*12, 13*). The insensitivity of the surface nickel oxide Raman band to the presence of moisture on the sample surface (Fig. 2a vs 2d) suggests that water molecules do not coordinate to the supported nickel oxide. Yet, the combined LRS, TPR, and XPS data suggest the supported nickel oxide is present as a highly dispersed surface oxide on the alumina support. The pronounced thermal broadening of the supported nickel oxide Raman band at elevated temperatures (Figs. 2b and c) suggests that the nickel oxide vibrational modes may be intimately coupled to the vibrations of the alumina support. The water insensitivity of the supported nickel oxide and the pronounced thermal broadening of the Raman band at elevated temperatures are consistent with the incorporation of the nickel oxide into the defects of the γ-Al_2O_3 surface. Ion scattering spectroscopy is uniquely sensitive to the outermost layers of a sample and confirms that the Ni^{2+} is present in the surface region of the alumina support (*14*). Additional support for the conclusion that surface nickel oxide is incorporated into the subsurface of the alumina support is found in earlier reflectance studies by Lo Jacono *et al.* (*15*) and Cimino *et al.* (*16*) which showed that the nickel oxide supported on alumina is present as Ni^{2+} ions in a spinel-like phase in the surface of the alumina support (surface spinel).

The supported metal oxides previously studied with *in situ* laser Raman spectroscopy all possess high oxidation states (Re^{7+}, W^{6+}, Mo^{6+}, Cr^{6+}, and V^{5+}). The high oxidation states of these metal oxides cannot be accommodated in the γ-Al_2O_3 lattice and lead to oxide structures not compatible with the γ-Al_2O_3 structure (*10*). Thus, these metal oxides *adsorb* on the alumina support surface. Nickel oxide does not possess high oxidation states (*10*) and the XPS measurements reveal that it is present as Ni^{2+} when it interacts with γ-Al_2O_3. The low oxidation state of nickel oxide can be accommodated in the γ-Al_2O_3 lattice and leads to the formation of NiO–Al_2O_3 spinels (*10*). Thus, nickel oxide can be *absorbed* into the surface of the alumina support as a surface spinel. Heating the NiO/Al_2O_3 sample to 700°C causes the diffusion of the surface nickel oxide into the bulk of the alumina support (*17*).

The *in situ* laser Raman spectroscopy studies of supported metal oxides have revealed that there are two types of supported metal oxides on γ-alumina. Metal oxides that have high oxidation states (W^{6+}, Mo^{6+}, V^{5+}, Re^{7+}, and Cr^{6+}) are *adsorbed* on the surface of γ-alumina because they cannot be accommodated in the γ-Al_2O_3 lattice. The surface metal oxides belonging to this category usually possess strong Raman bands at ~900–1100 cm^{-1} associated with the terminal M=O bond (7), and are sensitive to the presence of water vapor. Metal oxides that have low oxidation states (Ni^{2+}, Cu^{2+}, and Co^{2+}) are *absorbed* into the surface of the alumina support as a surface spinel because they can be accommodated in the γ-Al_2O_3 lattice. The surface metal oxides belonging to this category usually possess Raman bands at ~300–800 cm^{-1} (*17*) and are not sensitive to the presence of water vapor. Thus, *in situ* laser Raman spectroscopy studies are capable of distinguishing between metal oxides that are adsorbed on the alumina support and metal oxides that appear to be absorbed into the alumina support surface as a surface spinel.

ACKNOWLEDGMENTS

The authors would like to thank W. Mykytka for the preparation of the NiO catalyst, S. Soled for the preparation of the $NiAl_2O_4$ sample, and F. D. Hardcastle for critical discussions.

REFERENCES

1. Chan, S. S., Wachs, I. E., Murrell, L. L., Wang, L., and Hall, W. K., *J. Phys. Chem.* **88,** 5831 (1984).
2. Wachs, I. E., and Chan, S. S., *Appl. Surf. Sci.* **20,** 181 (1984).
3. Stencel, J. M., Makovsky, L. E., Sarkus, T. A., DeVries, J., Thomas, R., and Moulijn, J. A., *J. Catal.* **90,** 314 (1984).
4. Stencel, J. M., Makovsky, L. E., Diehl, J. R., and Sarkus, T. A., *J. Raman Spectrosc.* **15,** 282 (1984).
5. Wang, L., and Hall, W. K., *J. Catal.* **82,** 177 (1983).
6. Wang, L., Ph.D. thesis. University of Wisconsin–Milwaukee (1982).
7. Beatie, I. R., and Gilson, T. R., *J. Chem. Soc. A,* 2322 (1969).
8. Chan, S. S., and Bell, A. T., *J. Catal.* **89,** 433 (1984).
9. Chan, S. S., Wachs, I. E., Murrell, L. L., and Dispenziere, N., *J. Catal.* **92,** 1 (1985).
10. Wells, A. F., "Structural Inorganic Chemistry," 5th ed. Oxford Univ. Press (1984).
11. Chan, S. S., Wachs, I. E., and Saleh, R. Y., to be published.
12. Dietz, R. E., Parisot, G. I., and Meixner, A. E., *Phys. Rev., B: Condens. Matter* **4,** 2302 (1971).
13. Perry, C. H., Anastassakis, E., and Sokoloff, J., *Indian J. Pure Appl. Phys.* **9,** 930 (1971).
14. Wu, M., and Hercules, D. M., *J. Phys. Chem.* **83,** 2003 (1979).
15. Lo Jacono, M., Schiavello, M., and Cimino, A., *J. Phys. Chem.* **75,** 1044 (1971).
16. Cimino, A., Lo Jacono, M., and Schiavello, M., *J. Phys. Chem.* **79,** 243 (1975).
17. Hardcastle, F. D., and Wachs, I. E., to be published.

SHIRLEY S. CHAN[1]
ISRAEL E. WACHS[2]

Corporate Research-Science Laboratories
Exxon Research and Engineering Company
Annandale, New Jersey 08801

Received October 22, 1985

---

[1] Present address: The BOC Group, Technical Center, 100 Mountain Avenue, Murray Hill, N.J. 07974.

[2] To whom correspondence should be addressed.